Mono-, di- and tetra-nuclear ruthenium(II) complexes containing 2,2′-*p*-phenylenebis(imidazo[4,5-*f*]phenanthroline): synthesis, characterization and third-order non-linear optical properties

Hui Chao,[a] Run-Hua Li,[a] Cai-Wu Jiang,[a] Hong Li,[a] Liang-Nian Ji *[acd] and Xiao-Yuan Li *[b]

[a] *State Key Laboratory of Ultrafast Laser Spectroscopy/Department of Chemistry, Zhongshan University, Guangzhou 510275, P. R. China. E-mail: cesjln@zsu.edu.cn*
[b] *Department of Chemistry, Hong Kong University of Science and Technology, Kowloon, Hong Kong, P. R. China. E-mail: chxyli@ust.hk*
[c] *State Key Laboratory of Coordination Chemistry, Nanjing University, Nanjing 210093, P. R. China*
[d] *State Key Laboratory of Bio-organic and Natural Products Chemistry, Shanghai Institute of Organic Chemistry, Shanghai 200032, P. R. China*

Received 15th February 2001, Accepted 12th April 2001
First published as an Advance Article on the web 21st May 2001

Mono-, di- and tetra-nuclear ruthenium(II) complexes containing 2,2′-*p*-phenylenebis(imidazo[4,5-*f*]phenanthroline) (H_2bpib) have been synthesized and characterized. Electrochemical and UV/Vis data show that the first redox process in these complexes is bipyridine based and the metal–metal interaction in di- and tetra-nuclear complexes is very weak. Resonance Raman spectra provide direct evidence for a low-energy bipyridine to H_2bpib charge-transfer transition. Furthermore, the non-linear optical properties of the ruthenium(II) complexes were investigated by *Z*-scan techniques with 12 ns laser pulses at 540 nm, and all of them exhibit both NLO absorption and self-defocusing effect. The corresponding effective NLO susceptibilities $|\chi^3|$ of the complexes are 5.76×10^{-12}–21.06×10^{-12} esu.

In the last few years organometallic and coordination complexes have been the subject of active study as non-linear optical (NLO) materials.[1,2] Compared to organic molecules, metal complexes can have a larger variety of structures with comparable or, in some cases, higher environmental stability and a much greater diversity of tunable electronic properties by virtue of the metal center. Incorporation of metals into NLO systems opens up possibilities unavailable with purely organic materials. However, the vast majority of such studies have been focused on quadratic optical non-linearities and, to a far lesser extent, on third-order responses. Until now, the design of second-order NLO materials follows some well defined guidelines, but the structure–property relationships that govern third-order NLO polarization are a little vague. Only some complexes with large π-conjugated systems have been observed to exhibit large third-order non-linearities.[3–5]

Recent studies[5–11] indicate that ruthenium complexes are promising candidates for NLO materials because of their rich photochemical properties and varied coordination. We have also recently discovered that mononuclear ruthenium(II) complexes containing 2-phenylimidazo[4,5-*f*][1,10]phenanthroline derivatives show large third-order NLO effects.[12] It is known that polynuclear complexes possess larger π-conjugated systems in comparison with mononuclear complexes, and this may be helping to achieve larger third-order NLO responses. A similar case has been observed when exploring the NLO potential of π-delocalized alkynylruthenium dendrimers.[5] Although the number of investigations concerning the photochemical and photophysical behavior of dinuclear or polynuclear ruthenium(II) polypyridine complexes is rapidly growing, to our knowledge there are no reports on the third-order NLO properties of them. In order to construct polynuclear complexes with third-order non-linearities, we have designed a new bridging ligand which is derived from 2-phenylimidazo[4,5-*f*][1,10]phenanthroline. Herein we report its synthesis and present the preparation, characterization and third-order NLO properties of corresponding ruthenium(II) complexes.

Experimental

Syntheses

The compounds $[Ru(bpy)_2Cl_2]\cdot 2H_2O$[13] and 1,10-phenanthroline-5,6-dione (phendione)[14] were synthesized according to literature methods. All other reagents were obtained commercially and used as supplied.

2-(4-Formylphenyl)imidazo[4,5-*f*][1,10]phenanthroline (fmp). A mixture of terephthalic aldehyde (0.201 g, 1.5 mmol), 1,10-phenanthroline-5,6-dione (0.315 g, 1.5 mmol), ammonium acetate (2.31 g, 30 mmol) and glacial acetic acid (30 cm^3) was refluxed for about 2 h, then cooled to room temperature and diluted with water (*ca.* 60 cm^3). Dropwise addition of concentrated aqueous ammonia gave a yellow precipitate, which was collected and washed with water. The crude product in ethanol was purified by silica gel filtration (60–100 mesh, ethanol). The principal yellow band was collected. The yellow crystalline solid obtained by slow evaporation of the solution was dried *in vacuo*. Yield 0.351 g, 72.3% (Found: C, 70.1; H, 4.0; N, 16.1. $C_{20}H_{12}N_4O\cdot H_2O$ requires C, 70.2; H, 4.1; N, 16.4%). $\tilde{\nu}_{max}/cm^{-1}$: 3374m, 3064s, 1693s, 1609m, 1567m, 1482m, 1398m, 807s and 737s. ^1H NMR data (DMSO-d^6): δ 13.85 (s, 1H), 10.09 (s, 1H), 9.04 (d, 2H), 8.94 (d, 2H), 8.51 (d, 2H), 8.13 (d, 2H), 7.84 (q, 2H). FAB-MS: $m/z = 325$ ($C_{20}H_{12}N_4O$ requires 324).

2,2′-*p*-Phenylene(imidazo[4,5-*f*][1,10]phenanthroline (H_2bpib). A mixture of 1,10-phenanthroline-5,6-dione (0.63 g, 3 mmol), ammonium acetate (4.62 g, 60 mmol), terephthalic aldehyde (0.201 g, 1.5 mmol) and glacial acetic acid (50 cm^3) was refluxed for about 2 h then cooled to room temperature.

DOI: 10.1039/b101483h

The precipitate was collected and washed with water. The crude product was recrystallized from DMF and produced a greenish yellow powder. Yield 0.154 g, 20% (Found: C, 74.33; H, 3.33; N, 21.56. $C_{32}H_{18}N_8$ requires C, 74.71; H, 3.50; N, 21.79%). $\tilde{\nu}_{max}$/cm^{-1}: 3423s, 3177m, 1616m, 1567m, 1475m, 1454s, 1384m, 807s and 737s. ^{1}H NMR data (DMSO-d^6): δ 13.97 (s, 2H), 9.08 (d, 4H), 8.98 (d, 4H), 8.54 (s, 4H), 7.83 (q, 4H). FAB-MS: *m*/*z* = 515 ($C_{32}H_{18}N_8$ requires 514).

[Ru(bpy)$_2$(fmp)][ClO$_4$]$_2$ 1. A mixture of [Ru(bpy)$_2$Cl$_2$]·2H$_2$O (0.261 g, 0.5 mmol), fmp (0.162 g, 0.5 mmol), methanol (20 cm^3) and water (10 cm^3) was refluxed for 5 h to give a clear red solution. After most of the ethanol was removed by rotatory evaporation, a red precipitate was obtained by dropwise addition of aqueous $NaClO_4$ solution. The crude product was purified by recrystallization by diffusion of diethyl ether into the acetonitrile solution. Yield 0.413 g, 85% (Found: C, 49.26; H, 3.50; N, 11.47. $C_{40}H_{28}Cl_2N_8O_9Ru\cdot 2H_2O$ requires C, 49.38; H, 3.32; N, 11.52%). $\tilde{\nu}_{max}$/cm^{-1}: 3430w (br), 3071w, 1693m, 1651m, 1602m, 1440m, 1082vs (ClO_4), 807m, 765s, 723m and 625s. ^{1}H NMR [$(CD_3)_2SO$]: δ 10.18 (s, 1H), 8.96 (d, 2H), 8.87 (d, 2H), 8.84 (d, 2H), 8.52 (d, 2H), 8.24 (t, 2H), 8.15 (d, 2H), 8.10 (t, 2H), 8.05 (d, 2H), 8.02 (d, 2H), 7.89 (d, 2H), 7.77 (dd, 2H), 7.61 (t, 2H), 7.38 (t, 2H). FAB-MS: *m*/*z* = 837 (M − ClO_4) and 737 (M − 2ClO_4). The chloride salt was prepared from the perchlorate by precipitation in acetone solution with tetra-*n*-butylammonium chloride.

[Ru(bpy)$_2$(H$_2$bpib)][ClO$_4$]$_2$ 2. A solution of [Ru(bpy)$_2$-(fmp)]Cl$_2$ (0.323 g, 0.4 mmol) in glacial acetic acid (5 cm^3) was added dropwise under argon to a mixture of 1,10-phenanthroline-5,6-dione (0.084 g, 0.4 mmol) and ammonium acetate (0.616 g, 8 mmol) in glacial acetic acid (5 cm^3). The mixture was refluxed under argon for 2 h. After neutralization with concentrated aqueous ammonia, a red precipitate was obtained by dropwise addition of aqueous $NaClO_4$ solution. The product was purified by column chromagraphy on alumina with acetonitrile as eluent and dried *in vacuo*. Yield: 0.293 g, 65% (Found: C, 54.83; H, 3.02; N, 14.98. $C_{52}H_{34}Cl_2N_{12}O_8Ru\cdot H_2O$ requires C, 54.54; H, 3.15; N, 14.68%). $\tilde{\nu}_{max}$/cm^{-1} 3395w (br), 3064w, 1623m, 1602m, 1447m, 1082vs (ClO_4), 807m, 765s, 723m and 625s. ^{1}H NMR [$(CD_3)_2SO$]: δ 14.37 (s, 1H), 13.85 (s, 1H), 9.01 (d, 2H), 8.94 (d, 2H), 8.87 (d, 2H), 8.84 (d, 2H), 8.76 (d, 2H), 8.51 (s, 4H), 8.22 (t, 2H), 8.07 (d, 2H), 7.87 (m, 4H), 7.77 (br, 4H), 7.61 (t, 2H), 7.39 (t, 2H). FAB-MS: *m*/*z* = 1028 (M − ClO_4) and 928 (M − 2ClO_4).

[(bpy)$_2$Ru(H$_2$bpib)Ru(bpy)$_2$][ClO$_4$]$_4$ 3. A solution of [Ru-(bpy)$_2$Cl$_2$]·2H$_2$O (0.25 g, 0.58 mmol) in glycerol was heated under argon for 30 min. Solid H$_2$bpib (0.149 g, 0.29 mmol) was added to the reddish violet solution, and the resulting mixture refluxed for 12 h, turning dark red. It was cooled to room temperature, and 60 cm^3 water were added. After filtration, a dark red precipitate was obtained by dropwise addition of aqueous $NaClO_4$ solution. The product was purified by column chromatography on alumina with acetonitrile–ethanol (4 : 1 v/v) as eluent. Yield: 0.392 g, 77.8% (Found: C, 47.92; H, 3.16; N, 12.31. $C_{72}H_{50}Cl_4N_{16}O_{16}Ru_2\cdot 3H_2O$ requires C, 48.21; H, 3.12; N, 12.49%). $\tilde{\nu}_{max}$/cm^{-1} 3395w (br), 3064w, 1602m, 1447m, 1082vs (ClO_4), 807m, 765s, 723m and 625s. ^{1}H NMR [$(CD_3)_2SO$]: δ 9.13 (d, 4H), 8.88 (d, 4H), 8.84 (d, 4H), 8.58 (s, 4H), 8.23 (t, 4H), 8.11 (t, 4H), 8.00 (br, 4H), 7.89 (br, 4H), 7.87 (d, 4H), 7.63 (d, 4H), 7.60 (t, 4H), 7.37 (t, 4H). ES-MS [CH_3OH]: *m*/*z* 769.7 ([M − 2ClO$_4$]$^{2+}$), 478.8 ([M − 3ClO$_4$]$^{3+}$), 446.9 ([M − 4ClO$_4$ − H]$^{3+}$), 335.7 ([M − 4ClO$_4$]$^{4+}$).

[Ru{(bpy)$_2$Ru(H$_2$bpib)}$_3$][ClO$_4$]$_8$ 4. A suspension of RuCl$_3$·3H$_2$O (0.026 g, 0.1 mmol) in 20 cm^3 of glycerol was stirred at 100 °C under argon for 1.5 h turning green. Then [Ru(bpy)$_2$-(H$_2$bpib)][ClO$_4$]$_2$·H$_2$O (0.343 g, 0.3 mmol) was added, and the solution temperature maintained at 120 °C for 24 h. The solution was cooled to room temperature, and 60 cm^3 water were added. After filtration, a dark red precipitate was obtained by dropwise addition of aqueous $NaClO_4$ solution. The product was purified by SP-Sephadex C-25 cation exchange chromatography with a solution 0.5 M NaCl in water–acetone (5 : 3) as eluent. Yield 0.237 g, 63.6% (Found: C, 49.71; H, 3.36; N, 13.13. $C_{156}H_{102}Cl_8N_{36}O_{32}Ru_4\cdot 3H_2O$ requires C, 50.16; H, 2.89; N 13.50%). ^{1}H NMR [$(CD_3)_2SO$]: δ 9.17 (br, 12H), 8.87 (d, 6H), 8.83 (d, 6H), 8.63 (s, 12H), 8.23 (t, 6H), 8.11 (m, 18H), 7.97 (br, 12H), 7.86 (d, 6H), 7.63 (d, 6H), 7.60 (t, 6H), 7.36 (t, 6H). ES-MS [CH_3O]: *m*/*z* 769.8 ([M − 6ClO$_4$ − 2H]$^{4+}$), 720 ([M − 8ClO$_4$ − 4H]$^{4+}$), 480.9 ([M − 8ClO$_4$ − 2H]$^{6+}$), 412 ([M − 8ClO$_4$ − H]$^{7+}$), 360.9 ([M − 8ClO$_4$]$^{8+}$).

CAUTION: perchlorate salts of metal complexes with organic ligands are potentially explosive, and only small amounts of the material should be prepared and handled with great care.

Physical measurements

Microanalyses (C, H and N) were carried out with a Perkin-Elmer 240Q elemental analyzer. Infrared spectra were recorded on a Nicolet 170SX-FTIR spectrometer as KBr discs, US/VIS spectra on a Shimadzu MPS-2000 spectrophotometer, ^{1}H NMR spectra on a Varian 500 MHz NMR spectrometer with $(CD_3)_2SO$ as solvent at room temperature and $SiMe_4$ as an internal standard and fast atomic bombardment mass spectra (FAB-MS) on a VG ZAB-HS spectrometer in a 3-nitrobenzyl alcohol matrix. Electrospray mass spectra (ES-MS) were recorded on a LCQ system (Finngan MAT, USA) using methanol as mobile phase. The spray voltage, tube lens offset, capillary voltage and capillary temperature were set at 4.50 kV, 30.00 V, 23.00 V and 200 °C, respectively, and the quoted *m*/*z* values are for the major peaks in the isotope distribution.

Resonance Raman spectra were obtained with various excitations from a Coherent INNOVA-400 Kr$^+$ or Ar$^+$ CW laser. A Spex-1403 double monochromator equipped with an electrically cooled photomultiplier was used to collect Raman scattering with a 1 cm^{-1} s^{-1} scan rate and 1 s per step. The slit width of the monochromator was set such that the spectral resolution is ≈4 cm^{-1}. Spectra were obtained *via* 90° scattering geometry from a spinning liquid cell or from a 1 mm diameter capillary tube. Pyridine was used as the primary solvent to dissolve the compound, followed by transfer of the pyridine solution to a silver sol freshly prepared using the standard citrate reduction method and aggregated using 0.5 M KCl. Off-resonance FT-Raman spectra were obtained on a Bruker IFS-66 Raman spectrometer from a KBr pellet of the sample. Typically, a 1 : 150 ratio in weight between sample and dry KBr was used to prepare the pellet. A Ge/SiO$_2$ beam splitter and a liquid N$_2$ cooled germanium detector were used for Raman measurements. For the sample, 1000 scans were collected and added in FT-Raman measurement.

Cyclic voltammetry was performed on an EG&G PAR 273 polarographic analyser and 270 universal programmer. The supporting electrolyte was 0.1 M tetrabutylammonium perchlorate in acetonitrile freshly distilled from phosphorus pentaoxide and deaerated by purging with nitrogen. A standard three-electrode system was used comprising a platinum microcylinder working electrode, platinum-wire auxiliary electrode and a saturated calomel reference electrode (SCE).

Non-linar optical measurements

Acetonitrile solutions of 5.0×10^{-5} M of the ruthenium complexes were placed in a 2 mm quartz cuvette for optical measurements. Their non-linear refraction and absorption were measured with a linearly polarized laser light (λ = 540 nm; pulse width (FWHM) = 12 ns) generated from an excimer laser (Lambda Physics EMG 201MSC)-pumped dye laser (Lambda

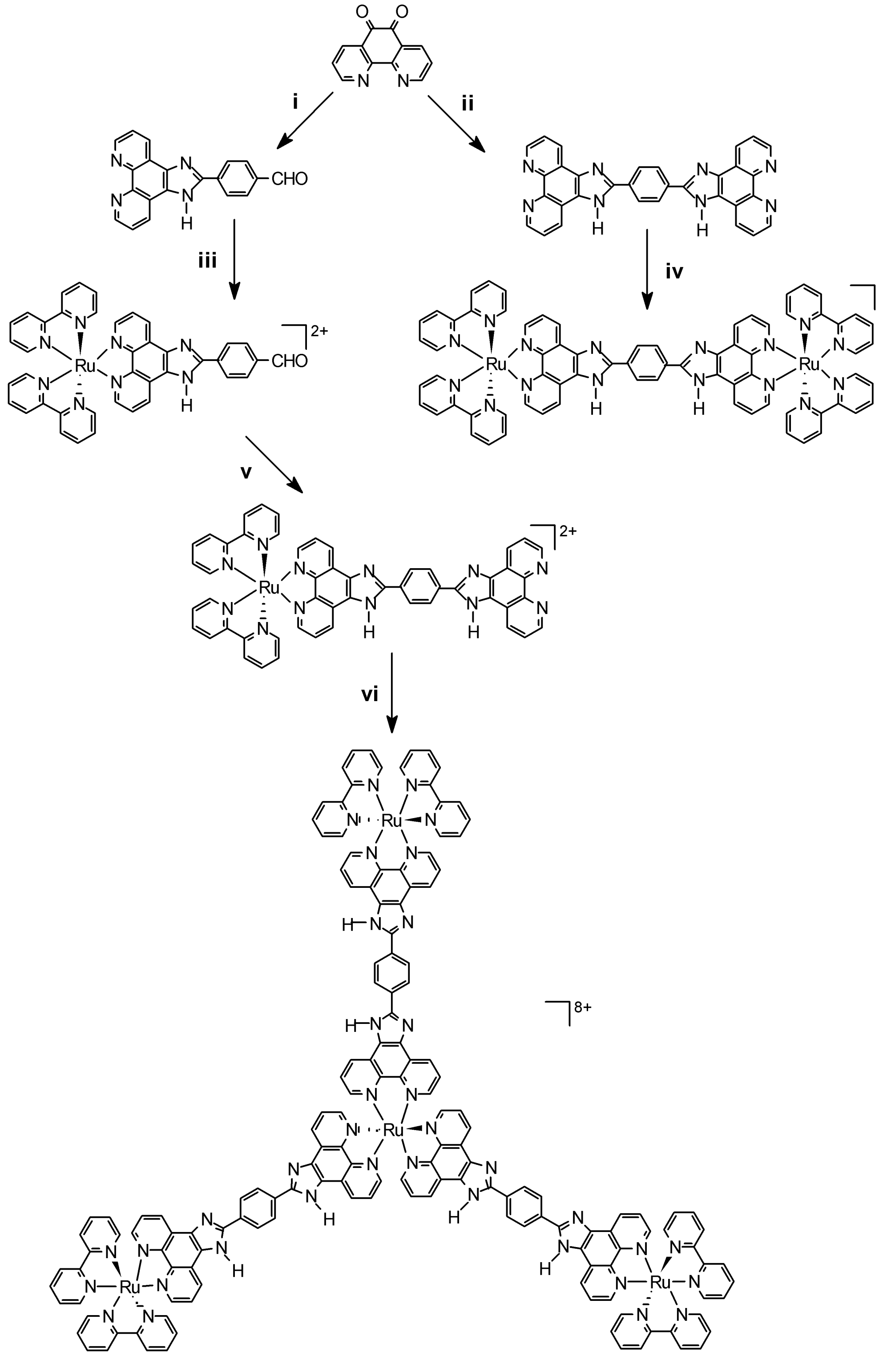

Scheme 1 Synthetic routes for the preparation of the ligands and complexes: (i) 1 equivalent terephthalic aldehyde, (ii) 2 equivalents terephthalic aldehyde, (iii) [Ru(bpy)$_2$Cl$_2$], (iv) [Ru(bpy)$_2$Cl$_2$], (v) phendione, (vi) RuCl$_3$.

Physics model FL2002) system. The spatial profiles of the optical pulses were nearly Gaussian. The laser beam was focused with a 5 cm focal-length focusing mirror. The radius of the beam waist at focus point was measured to be 30 μm (half-width at 1/e^2 maximum). The repetition rate of the laser pulse is 10 Hz. The incident and transmitted pulse energy were measured by a Laser Precision detector (RJ-7200 energy probe). The NLO properties of the samples were manifested by moving the samples along the axis of the incident beam (Z direction) with respect to the focal point. An aperture of 0.5 mm radius was placed in front of the detector to assist the measurement of the self-defocusing effect.

Results and discussion

Syntheses

An outline of the synthesis of the ligands and complexes is presented in Scheme 1. The ligands were synthesized on the basis of the method for imidazole ring preparation established by Steck and Day.[15] The ligands 2-(4-formylphenyl)imidazo-[4,5-*f*][1,10]phenanthroline (fmp) and 2,2′-*p*-phenylenebis-(imidazo[4,5-*f*]phenanthroline) (H$_2$bpib) were obtained through condensation of 1,10-phenanthroline-5,6-dione (phendione) with terephthalic aldehyde in refluxing glacial acetic acid containing ammonium acetate at a molar ratio of

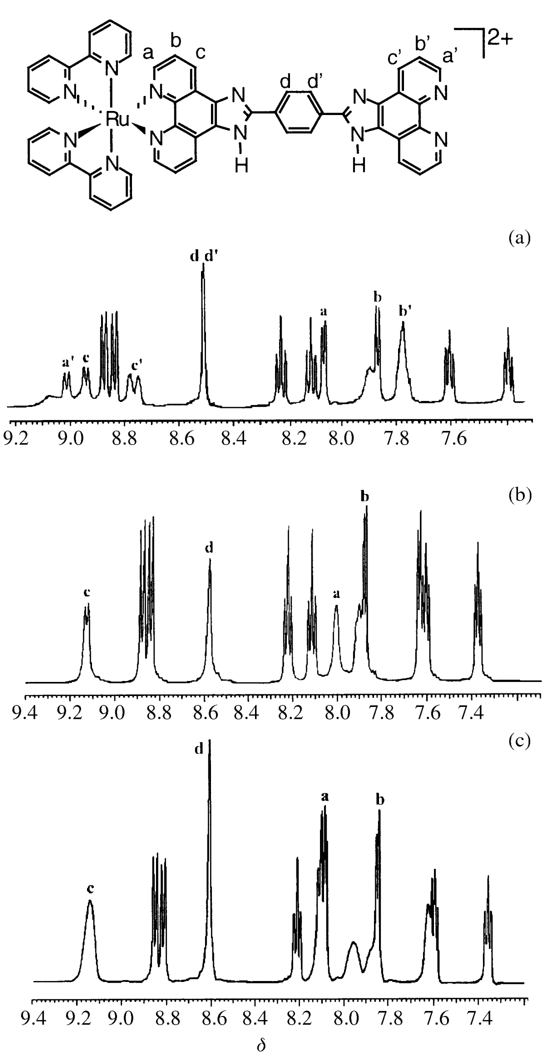

Fig. 1 ^1H NMR spectra of $[Ru(bpy)_2(H_2bpib)]^{2+}$ (a), $[(bpy)_2Ru(H_2bpib)Ru(bpy)_2]^{4+}$ (b) and $[Ru\{(bpy)_2Ru(H_2bpib)\}_3]^{8+}$ (c) in the aromatic region between δ 7.3 and 9.4 [$(CD_3)_2SO$ solvent, TMS reference].

Table 1 Redox potentials for the ruthenium(II) complexes[a]

Complex	Ru^{III}/Ru^{II}		Ligand reduction	
2	1.27		−1.43	−1.68
3	1.27 (2e⁻)		−1.40 (2e⁻)	−1.65 (2e⁻)
4	0.83	1.25 (3e⁻)	−1.38 (3e⁻)	−1.65 (3e⁻)

[a] All complexes were measured in 0.1 M NBu_4ClO_4–CH_3CN, error in potentials ±0.02 V; $T = 23 \pm 1$ °C; scan rate = 100 mV s^{-1}.

1 : 1 or 2 : 1, respectively. The ligand H_2bpib is sparingly soluble in common organic solvents, but partly soluble in hot DMF and DMSO. This prevents efficient synthesis of the mononuclear complex **2** since it is much more soluble than the ligand H_2bpib. Even when the reaction between $[Ru(bpy)_2Cl_2]$ and H_2bpib was run in a 1 : 1 molar ratio in glycerol, only the dinuclear complex **3** was formed. Therefore, to prepare the mononuclear complex **2**, we have carried out the condensation of 1,10-phenanthroline-5,6-dione with the pre-coordinated fmp in $[Ru(bpy)_2(fmp)]^{2+}$ **1** to avoid the formation of the dinuclear complex (Scheme 1). The reaction of $RuCl_3$ with three equivalents of the mononuclear complex **2** in glycerol afforded the tetranuclear complex **4**. All these complexes were purified by column chromatography and characterized by IR, ^1H NMR, MS and elemental analyses.

^1H NMR Spectra

Assignments of the ^1H NMR spectra of these new compounds were made by comparison with those of similar compounds[16–18] and confirmed by ^1H–^1H COSY experiments. The proton on the nitrogen atom of the imidazole resonates at *ca.* δ 13.97 for the free ligand H_2bpib as a broad singlet, but it is unobserved for the ruthenium complexes because of its quickly exchanging between the two nitrogens of the imidazole ring, characteristic of an active proton. So the bridging ligand and the complexes all exhibit C_2 symmetry in NMR experiments. As a consequence, the two halves of H_2bpib are chemically and magnetically equivalent. In the ^1H NMR spectrum of free H_2bpib the proton signals at δ 13.97, 9.08, 8.98, 8.54 and 7.83 can easily be assigned to H(NH), H_a, H_c, H_d and H_b respectively.

It is easy to assign the chemical shifts of the protons of the bridging ligand H_2bpib in its complexes bearing in mind the free H_2bpib data. The ^1H NMR spectra for complexes **2**, **3** and **4** are shown in Fig. 1. On coordination to two ruthenium ions to form complex **3**, the protons on the H_2bpib all experience large shifts except H_b and H_d by comparison with those of free H_2bpib: H_c shows 0.15 ppm downfield shifts while H_a experiences surprising upfield shifts of 1.08 ppm. Similar behaviors are also observed for complex **4**. For the dinuclear and tetranuclear complexes only the coordinated H_2bpib resonances are observed, whereas for the mononuclear complex **2** two distinct sets of aromatic resonances for both coordinated and uncoordinated parts of H_2bpib are observed; the upfield shift is especially clear for H_a, which may be due to the effect of the ring current of the bpy ligands.

Electrochemistry

The electrochemical behaviors of the complexes have been studied in CH_3CN by cyclic voltammetry. Results are collected in Table 1. For each complex dissolved in acetonitrile only two reversible reduction waves are observed in the cyclic voltammogram between 0 and −1.8 V (*vs.* SCE). By comparing with the redox behaviors of $[Ru(bpy)_3]^{2+}$ and related complexes,[19–21] they are characteristic of the two bpy ligands. From the similarities in reduction behavior of all the three complexes, it has been concluded that the LUMO π* orbitals of mono-, di- and tetranuclear complexes reported here are bpy and not H_2bpib based.

The mononuclear complex **2** exhibits one reversible oxidation at +1.27 V, which is nearly equal with that of $[Ru(bpy)_3]^{2+}$. For the dinuclear complex **3** the oxidation potentials are not affected by the second complexation, it also exhibits one oxidation wave. No difference in the oxidation potential was observed between mono- and di-nuclear complexes (Table 1). Coulometry indicates that two electrons are involved in this process. From the separation between the anodic and cathodic peak potential (56 mV) it is concluded that two closely spaced one-electron processes are involved in this oxidation. By use of the Richardson and Taube approach,[22] the comproportionation constant K_c can be estimated for the dinuclear complex. The value is very near to the statistical limit, *i.e.* $K_c = 4$, indicating that in the present system the electrostatic interaction between metal sites plays a negligible role. This is attributed to the large separation between the two $Ru(bpy)_2$ units and free rotation around the C–C bond of H_2bpib.

Cyclic voltammograms of **4** show two revisible metal-based oxidations (in ratio 1 : 3). The first oxidation wave at 0.83 V involves one electron and is attributed to the central ruthenium atom. The second oxidation potential, at 1.25 V, is very close to those of the mono- and di-nuclear complexes. This three-electron oxidation wave can be attributed to simultaneous oxidations of the three terminal ruthenium centers. The results also confirm that the first redox process in these complexes is bipyridine based.

Absorption spectra

The absorption spectra of the complexes are shown in Fig. 2, and the energy maxima and absorption coefficients are

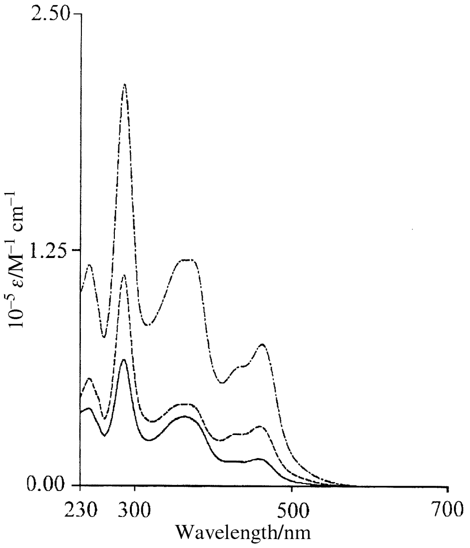

Fig. 2 Absorption spectra of complexes **2** (full line), **3** (broken line) and **4** (dot-dash line) in CH_3CN at room temperature.

Table 2 UV-Visible spectral data for the ruthenium(II) complexes[a]

Complex	λ_{max}/nm (ε/M^{-1} cm^{-1})			
2	459 (14400)	355 (19700)	286 (35500)	245 (28200)
3	459 (29700)	370 (39300)	287 (66200)	243 (38800)
4	463 (48600)	366 (78700)	287 (138700)	243 (70600)

[a] In CH_3CN, $T = 298 \pm 1$ K.

summarized in Table 2. The spectrum of complex **2** consists of three well resolved bands at 459, 355 and 286 nm in the range 200 to 700 nm. The bands at 286 and 355 nm are attributed to the π–π* (bpy) and π–π* (H_2bpib) intraligand transitions, respectively, by comparison with the spectrum of $[Ru(bpy)_3]^{2+}$.[23] The lowest energy band at 459 nm is assigned to metal–ligand charge transfer (MLCT) and consists of overlapping Ru(dπ)→H_2bpib(π*) and Ru(dπ)→bpy(π*) transitions. For mixed-ligand complexes the interpretation becomes more complex, since there are multiple $d\pi-\pi_1^*$ and $d\pi-\pi_2^*$ transitions. The Ru(dπ)→H_2bpib(π*) and Ru(dπ)→bpy(π*) transitions cannot be separated from one another as observed for other mixed-ligand diimine complexes.[24]

When the mononuclear complex **2** is treated with another ruthenium centre to form the dinuclear complex **3** the MLCT absorption maximum around 460 nm remains almost unaltered, except it becomes twice as intense compared to the mononuclear complex (Fig. 2). A similar behaviour is also observed for the tetranuclear complex **4**. This is sharp contrast to π-accepting bridging systems such as [1,4-bis(4′-methyl-2,2′-bipyridin-4-yl)buta-1,3-diene],[25] and dpp [2,3-bis(2-pyridyl)pyrazine].[26] A shift to longer wavelength of the MLCT band occurs when a mononuclear complex containing such a π-accepting ligand forms a dinuclear complex. This indicates that in the present H_2bpib system the metal–metal interaction is very weak and the metal centers function mainly as part of a polarizable bridge.

Resonance Raman (rR) spectra

From the above experiments it was concluded that in the H_2bpib system the LUMO of the mixed-ligand complexes is localized at the bipyridine ligand. In order to confirm this resonance Raman spectra of the dinuclear complex **3** (excitation at 413.1, 457.9, 476.5, 496.5, 514.1 nm, respectively) were obtained (Fig. 3). Such spectra are often used to assign electronic transitions.[27–31] If excitation takes place into an allowed electronic transition, the rR spectrum is characterized by strong rR effects for the vibrations of those bonds that are mostly affected by the electronic transition. Thus, excitation into an allowed Ru→π* (α-diimine) transition primarily affects the diimine bonds. As a result, enhancement of Raman intensity is normally observed for the symmetrical stretching modes of the α-diimine ligand. With this method also the presence of different electronic transitions within one absorption band can be detected and identified by studying the wavelength dependence of the rR spectra.[31]

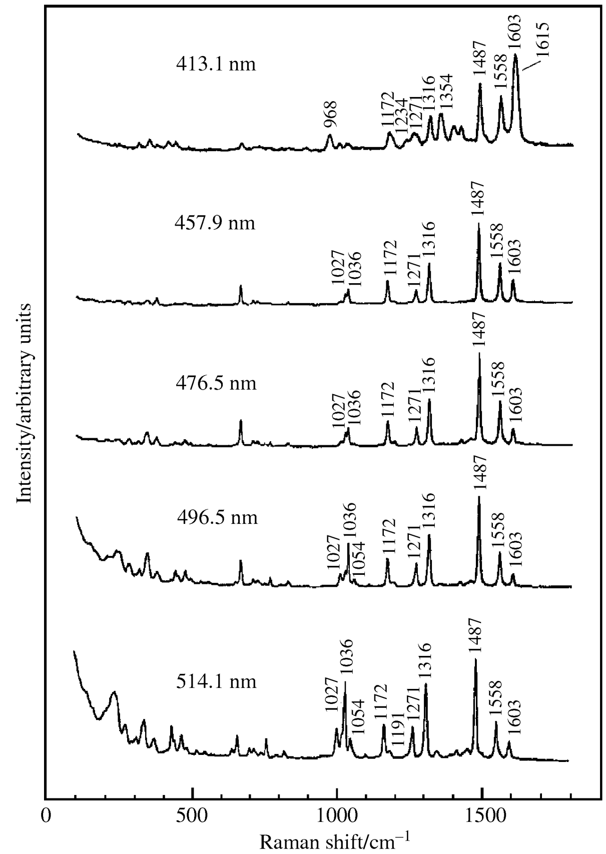

Fig. 3 Resonance Raman spectra of $[(bpy)_2Ru(H_2bpib)Ru(bpy)_2]^{4+}$ in a KBr pellet at room temperature at different excitation wavelengths.

Excitation with the 514.1 nm laser line at the low-energy side of the MLCT band of complex **3** ($\lambda = 459$ nm) gave rise to rR effects for ligand stretching modes at 1603, 1558, 1481, 1316, 1271, 1172, 1036 and 1027 cm^{-1}, which are in the same region as the bpy vibrations.[27–31] Excitation at 496.5, 476.5, 457.9 nm all yielded the same rR spectra, and again no H_2bpib vibrations were resonance enhanced. Only upon excitation with the 413.1 nm laser line at the high-energy side of the MLCT band H_2bpib vibrations were observed (1615, 1354, 1234 and 968 cm^{-1}). These results clearly show that, for complex **3**, much more bipyridine character is present at the low-energy side of the MLCT band. The resonance Raman measurements also indicate that in the H_2bpib system the first reduction potential is bipyridine-based, which is in agreement with the electrochemical measurements.

Non-linear optical properties

The non-linear optical properties of three ruthenium(II) complexes were investigated by *Z*-scan techniques[32–34] with 12 ns laser pulses at 540 nm, and all of them exhibit both non-linear optical refraction and non-linear optical absorption.

The non-linear absorption component was evaluated by *Z*-scan experiment under an open-aperture configuration (Fig. 4a). Light transmittance (T) is a function of the incident light irradiance $I_i(Z)$, non-linear absorption ($a_2 = a_2(I_i)$), and linear absorption (a_0) as illustrated in eqns. (1) and (2).[32,33] The

Table 3 Measurement results of the ruthenium(II) complexes using *Z*-scan techniques

Complex	$\Delta T_{\text{v-p}}$	$10^{-12}I_0$/ W m^{-2}	a/cm^{-1}	$10^{17}\,n_2$/m^2 W^{-1}	$10^{10}\,a_2$/m W^{-1}	$10^{12}\,\chi^{(3)a}$/esu	$10^{29a}\,\gamma$/esu
1	0.885	3.88	1.86	−1.67	0.94	5.76	7.34
2	0.924	3.46	4.12	−3.10	1.32	10.87	13.86
3	1.024	3.26	7.57	−5.99	2.75	21.06	26.85

[a] Errors are ±10%.

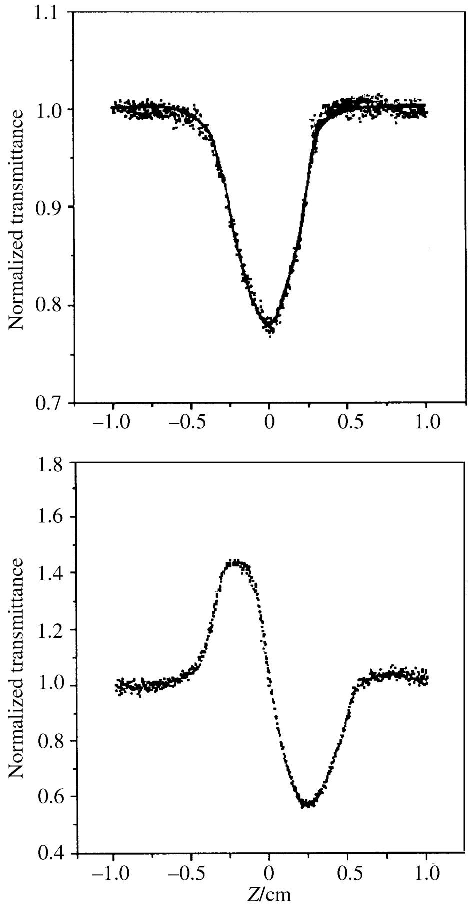

Fig. 4 *Z*-scan data (filled circles) of 5×10^{-5} M of $[\text{Ru}\{(\text{bpy})_2\text{Ru}(\text{H}_2\text{bpib})\}_3]^{8+}$, at 540 nm with I ($Z = 0$) being 3.26×10^{12} W m^{-2}: (a) collected under open-aperture configuration showing NLO absorption. The solid curve is a theoretical fit based on eqns. (1) and (2); (b) obtained by dividing the normalized *Z*-scan data obtained under closed-aperture configuration by the normalized *Z*-scan data in (a). It shows the self-defocusing effect of the complex.

$$T(Z) = \frac{1}{q(z)\sqrt{\pi}} \int_{-\infty}^{+\infty} \ln[1 + q(Z)]\exp(-\tau^2)\mathrm{d}\tau \qquad (1)$$

$$q(Z) = a_2 I_i(Z)\frac{(1 - e^{-a_0 L})}{a_0} \qquad (2)$$

a_2 value can be in turn determined by fitting a theoretical curve, $T(Z)$, to the *Z*-scan data according to eqns. (1) and (2). The solid line in Fig. 4(a) is a theoretical curve that fits best to the *Z*-scan data observed under the open-aperture configuration.

The non-linear refractive property of the ruthenium(II) complexes was assessed by dividing the normalized *Z*-scan data obtained under closed-aperture configuration by the normalized *Z*-scan data obtained under open-aperture configuration (Fig. 4b). This procedure helps to extract information on NLO refraction from a raw data set containing mixed information on both refraction and absorption.[33,34] The valley/peak pattern of the corrected transmittance curve so obtained shows characteristic self-defocusing behavior of propagating light in the sample.

An effective third-order non-linear refractive index n_2 can be derived from the difference between normalized transmittance values at the valley and peak ($\Delta T_{\text{v-p}}$) by eqn. (3), where n_2 is

$$n_2 = \frac{\lambda a_0}{0.812\pi I(1 - e^{-a_0 L})}\Delta T_{\text{v-p}} \qquad (3)$$

defined by $n = n_0 + n_2 I$. With measured values of $\Delta T_{\text{v-p}}$, a_0 and L, the n_2 value can be calculated. The values of a_2 and n_2 are listed in Table 3. In accordance with these, the modulus of the effective third-order susceptibility $\chi^{(3)}$ can be calculated by eqn. (4),[35] where λ is the wavelength of the laser (540 nm). The

$$|\chi^{(3)}| = \sqrt{\left|\frac{c\lambda n_0^2}{64\pi^3}a_2\right|^2 + \left|\frac{cn_0^2}{16\pi^2}n_2\right|^2} \qquad (4)$$

corresponding modulus of the hyperpolarizability γ can be obtained from $|\chi^{(3)}| = (1/3)N(n_o^2 + 2)^4|\gamma|$, where N is the compound concentration (in cm^{-3}) and n_o is the linear index of refraction of the complexes. The values of $|\chi^{(3)}|$ and $|\gamma|$ are also listed in Table 3.

It should be noted that the *Z*-scan measurements reported here could not reveal the origins of the observed non-linearities. Excited state effects, two-photon absorption, third-order bound-electronic effect and non-linear scattering can be responsible for the measured NLO effects.[36–38] The existing experimental data are insufficient to allow identification of the relative contributions of these mechanisms. Although the NLO parameters derived in this paper should be regarded as effective parameters only, the γ values obtained for the new complexes are large, and comparable with those of some known NLO chromophores (5.6×10^{-35}–8.6×10^{-34} esu for Group 10 metal alkynyl polymers at 1064 nm,[4] 2.27×10^{-32} esu for a alkynyl-ruthenium dendrimer at 800 nm,[5] 1.6×10^{-28} esu for half-open cubane-like $[\text{WOS}_3(\text{CuBr})_3(\mu\text{-Br})]^{3-}$ at 532 nm[39]). In particular, progressing from a mononuclear to tetranuclear complex results in a significant increase in γ. The overall magnitude of γ of the tetranuclear complex is approximately fourfold that of the mononuclear complex, indicating an additive contribution of relevant Ru(bpy)_3^{2+}-like NLO chromophores to the non-linearities of the polynuclear molecule.

Acknowledgements

We are grateful to the National Natural Science Foundation of China, the State Key Laboratory of Coordination Chemistry in Nanjing University and the State Key Laboratory of Bio-organic and Natural Products Chemistry in Shanghai Institute of Organic Chemistry for their financial support.

References

1 S. R. Marder, in *Inorganic materials*, eds. D. W. Bruce and D. O'Hare, Wiley, Chichester, 1992; D. R. Kanis, M. A. Ratner and T. J. Marks, *Chem. Rev.*, 1994, **94**, 195.

2 H. S. Nalwa, *Appl. Organomet. Chem.*, 1991, **5**, 349; N. J. Long, *Angew. Chem., Int. Ed. Engl.*, 1995, **34**, 21; T. Verbiest, S. Houbrechts, M. Kauranen, K. Clays and A. Persoons, *J. Mater. Chem.*, 1997, **7**, 2175; I. R. Whittall, A. M. McDonagh, M. G. Humphrey and M. Samoc, *Adv. Organomet. Chem.*, 1998, **42**, 291; H. Le Bozec and T. Renouard, *Eur. J. Inorg. Chem.*, 2000, 229.

3 W. J. Blau, H. J. Byrne, D. J. Cardin and A. P. Davey, *J. Mater. Chem.*, 1991, **1**, 245.

4 J. S. Shirk, J. R. Lindle, F. J. Bartoli, Z. H. Kafafi and A. W. Snow, in *Materials for Non-linear Optics*, eds. S. R. Marder, J. E. Sohn and G. D. Stucky, American Chemical Society, Washington, 1992, p. 626.

5 A. M. McDonagh, M. G. Humphrey, M. Samoc, B. Luther-Davies, S. Houbrechts, T. Wada, H. Sasabe and A. Persoons, *J. Am. Chem. Soc.*, 1999, **121**, 1405; A. M. McDonagh, M. G. Humphrey, M. Samoc and B. Luther-Davies, *Organometallics*, 1999, **18**, 5195.

6 W. M. Laidlaw, R. G. Denning, T. Verbiest, E. Chauchard and A. Persoons, *Nature* (*London*), 1993, **363**, 58; *Proc. SPIE-Int. Soc. Opt. Eng.*, 1994, **2143**, 14; F. W. Vance and J. T. Hupp, *J. Am. Chem. Soc.*, 1999, **121**, 4047.

7 C. Dhenaut, I. Ledoux, I. D. W. Samuel, J. Zyss, M. Bourgault and H. Le Bozec, *Nature* (*London*), 1995, **374**, 339.

8 S. Houbrechts, K. Clays, A. Persoons, V. Cadierno, M. P. Gamasa and J. Gimeno, *Organometallics*, 1996, **15**, 5266; V. Cadierno, S. Conejero, M. P. Gamasa, J. Gimeno, I. Asselberghs, S. Houbrechts, K. Clays, A. Persoons, J. Borge and S. Garcia-Granda, *Organometallics*, 1999, **18**, 582.

9 B. J. Coe, J. P. Essex-Lopresti, J. A. Harris, S. Houbrechts and A. Persoons, *Chem. Commun.*, 1997, 1645; B. J. Coe, M. C. Chamberlain, J. P. Essex-Lopresti, S. Gaines, J. C. Jeffery, S. Houbrechts and A. Persoons, *Inorg. Chem.*, 1997, **36**, 3284; B. J. Coe, J. A. Harris, L. J. Harrington, J. C. Jeffery, L. H. Rees, S. Houbrechts and A. Persoons, *Inorg. Chem.*, 1998, **37**, 3391; B. J. Coe, S. Houbrechts, I. Asselberghs and A. Persoons, *Angew. Chem., Int. Ed.*, 1999, **38**, 366; B. J. Coe, *Chem. Eur. J.*, 1999, **5**, 2464.

10 I. Y. Wu, J. T. Lin, J. Luo, C. S. Li, C. Tsai, Y. S. Wen, C. C. Hsu, F. F. Yeh and S. Liou, *Organometallics*, 1998, **17**, 2188.

11 I. R. Whittall, M. G. Humphrey, A. Persoons and S. Houbrechts, *Organometallics*, 1996, **15**, 1935; I. R. Whittall, M. P. Cifuentes, M. G. Mark, B. Luther-Davies, M. Samoc, S. Houbrechts, A. Persoons, G. A. Heath and D. C. R. Hockless, *J. Organomet. Chem.*, 1997, **549**, 127.

12 H. Chao, R. H. Li, B. H. Ye, H. Li, X. L. Feng, J. W. Cai, J. Y. Zhou and L. N. Ji, *J. Chem. Soc., Dalton Trans.*, 1999, 3711.

13 B. P. Sullivan, D. J. Salmon and T. J. Meyer, *Inorg. Chem.*, 1978, **17**, 3334.

14 M. Yamada, Y. Tanaka, Y. Yoshimato, S. Kuroda and I. Shimao, *Bull. Chem. Soc, Jpn.*, 1992, **65**, 1006.

15 E. A. Steck and A. R. Day, *J. Am. Chem. Soc.*, 1943, **65**, 452.

16 B. H. Ye, X. M. Chen, T. X. Zeng and L. N. Ji, *Inorg. Chim. Acta*, 1995, **240**, 5.

17 R. B. Nair, E. S. Teng, S. L. Kirkland and C. J. Murphy, *Inorg. Chem.*, 1998, **37**, 139.

18 J. Z. Wu, B. H. Ye, L. Wang, L. N. Ji, J. Y. Zhou, R. H. Li and Z. Y. Zhou, *J. Chem. Soc., Dalton Trans.*, 1997, 1395.

19 A. Kirsch-De Mesmaeker, R. Nasielski-Hinkens, D. Maetens, D. Pauwels and J. Nasielski, *Inorg. Chem.*, 1984, **23**, 377.

20 E. Amouyal, A. Homsi, J.-C. Chambron and J.-P. Sauvage, *J. Chem. Soc., Dalton Trans.*, 1990, 1841.

21 P. J. Delaive, J. T. Lee, H. W. Sprintschnik, T. J. Meyer and D. G. Whitten, *J. Am. Chem. Soc.*, 1977, **99**, 7094.

22 D. E. Richardson and H. Taube, *Inorg. Chem.*, 1981, **20**, 1278.

23 G. M. Bryant, J. E. Fergusson and H. K. J. Powell, *Aust. J. Chem.*, 1971, **24**, 257.

24 C. H. Braunstein, A. D. Baker, T. C. Strekas and H. D. Gafney, *Inorg. Chem.*, 1984, **23**, 857; R. Sahai, L. Morgan and D. P. Rillema, *Inorg. Chem.*, 1988, **27**, 2495; J. R. Show, R. T. Webb and R. H. Scheml, *J. Am. Chem. Soc.*, 1990, **112**, 1117.

25 A. I. Baba, H. E. Ensleg and R. H. Schmehl, *Inorg. Chem.*, 1995, **34**, 1198.

26 W. R. Murphy, K. J. Brewer, G. Gettliffe and J. D. Petersen, *Inorg. Chem.*, 1989, **28**, 81.

27 R. Hage, J. G. Haasnoot, D. J. Stufkens, T. L. Snoeck, J. G. Vos and J. Reedijk, *Inorg. Chem.*, 1989, **28**, 1413; R. Hage, J. G. Haasnoot, J. Reedijk, R. Wang and J. G. Vos, *Inorg. Chem.*, 1991, **30**, 3263.

28 D. J. Stufkens, T. L. Snoeck and A. B. P. Lever, *Inorg. Chem.*, 1988, **27**, 953; F. Hartl, T. L. Snoeck, D. J. Stufkens and A. B. P. Lever, *Inorg. Chem.*, 1995, **34**, 3887.

29 M. K. Nazeeruddin, M. Grätzel, K. Kalyanasundaram, R. B. Girling and R. E. Hester, *J. Chem. Soc., Dalton Trans.*, 1993, 323.

30 S. M. Scott, K. C. Gordon and A. K. Burrell, *J. Chem. Soc., Dalton Trans.*, 1999, 2669.

31 P. C. Servaas, H. K. Van Dijk, T. L. Snoeck, D. J. Stufkens and A. Oskam, *Inorg. Chem.*, 1985, **23**, 4494; Y. Fuchs, S. Lofters, T. Dieter, W. Shi, R. Morgan, T. C. Strekas, H. Gafney and A. D. Baker, *J. Am. Chem. Soc.*, 1987, **109**, 2691.

32 M. Sherk-Bahae, A. A. Said and E. W. Van Stryland, *Opt. Lett.*, 1989, **14**, 955.

33 M. Sherk-Bahae, A. A. Said, T. H. Wei, D. J. Hagan and E. W. Van Stryland, *IEEE J. Quantum Electron.*, 1990, **26**, 760.

34 A. A. Said, M. Sherk-Bahae, D. J. Hagan, T. H. Wei, J. Wang, J. Young and E. W. Van Stryland, *J. Opt. Soc. Am. B.*, 1992, **9**, 405.

35 L. Yang, R. Dorsinville, Q. Z. Wang, P. X. Ye, R. R. Alfano, R. Zamboni and C. Taliani, *Opt. Lett.*, 1992, **17**, 323.

36 W. Ji, W. Xie, S. H. Tang and S. Shi, *Mater. Chem. Phys.*, 1995, **43**, 1.

37 M. Sheik-Bahae, D. C. Hutching, D. J. Hagan and E. W. Van Stryland, *Phys. Rev. Lett.*, 1991, **65**, 96.

38 K. Mansour, M. J. Soileau and E. W. Van Stryland, *J. Opt. Soc. Am. B*, 1992, **9**, 1100.

39 Z. R. Chen, H. W. Hou, X. Q. Xin, K. B. Yu, H. C. Zeng and S. Shi, *J. Phys. Chem.*, 1995, **99**, 8717.